Title
CHEMISORPTION GEOMETRY OF PYRIDINE ON Pt(lll) BY NEXAFS

Author
Johnson, A.L.

Publication Date
1985-02-01

Lawrence Berkeley Laboratory

UNIVERSITY OF CALIFORNIA

Materials & Molecular Research Division

Submitted to The Journal of Physical Chemistry

CHEMISORPTION GEOMETRY OF PYRIDINE ON Pt(111) BY NEXAFS

A.L. Johnson, E.L. Muetterties, J. Stöhr, and F. Sette

February 1985

Prepared for the U.S. Department of Energy under Contract DE-AC03-76SF00098

DISCLAIMER

LBL-18694

Chemisorption Geometry of Pyridine on Pt(111) by NEXAFS

Allen L. Johnson and E. L. Muetterties#

Lawrence Berkeley Laboratory and Department of Chemistry

University of California, Berkeley

Berkeley, CA 94720

J. Stöhr

Corporate Research Science Laboratories

EXXON Research and Engineering Company

Annandale, NJ 08801

F. Sette

AT and T Bell Laboratories

600 Mountain Ave.

Murray Hill, NJ 07974

Near edge x-ray absorption fine structure (NEXAFS) measurements were employed to investigate the temperature dependent geometry of pyridine chemisorbed on the Pt(111) surface. At saturation coverage a low temperature state with an apparent angle between the ring plane and the surface plane of 52 ± 6^{o} was observed. This state converts (at $T \leq 300K$) to a high temperature state with an angle between the ring plane and the surface plane of 74 ± 10^{o}. An alpha pyridyl surface state that drives the transformation is proposed.

deceased

INTRODUCTION:

There have been many recent investigations of pyridine chemisorption on well defined surfaces of group 8 metals,[1-15] motivated by interest in surface enhanced Raman spectroscopy of pyridine, and the suitability of pyridine as a model compound for studies of the relative importance of π verses lone pair bonding on metal surfaces. The literature includes studies of pyridine chemisorption on well characterized surfaces of nickel[1-4], copper[5-6], rhodium[7], palladium[8-9], silver[10-11], iridium[12], and platinum[13-15]. Here we report the geometry of pyridine chemisorbed on Pt(111), derived from Near Edge X-ray Absorption Fine Structure (NEXAFS) measurements.

Previous studies of pyridine chemisorption have revealed a dependence of the angle between the pyridine ring plane and the metal surface with both coverage and temperature. On both Ag(111)[11] and Ni(100)[4] surfaces temperature and coverage dependent orientations have been found: parallel to the surface for low temperatures and coverages but tilted with respect to the surface at higher temperatures or coverages. Tilted or perpendicular pyridine chemisorption states have in fact been suggested for all the surfaces studied[1-15]. However, the structural assignments are generally based on the observation of quenching of electronic transitions (such as π-π^* excitations), valence level shifts, vibrational assignments (i.e. HREELS), or symmetry arguments and as such are approximate or ambiguous i.e. they generally indicate whether the observed state is in a high symmetry state or (perhaps slightly) perturbed from a symmetric state. In contrast, for unsaturated molecules weakly perturbed by chemisorption the analysis of the polarization dependence of NEXAFS transitions of π symmetry allow the determination of the relative angle of the unsaturated system in a straightforward manner.

The NEXAFS technique has been described in detail previously[16]. Briefly, the sample is exposed to a monochromatic, linearly polarized beam of variable

energy X-rays. The X-ray absorption coefficient is measured as a function of both the X-ray energy and the angle between the electric field vector $\vec{E}$ and the surface in the energy region near the K edge of an atom (e.g., C or N) in the adsorbed molecules. Absorption in this region is dominated by transitions into states localized on the molecule - generally antibonding π^* states (π resonances) and pseudobound states of σ symmetry (σ resonances).

The energy position of the near edge resonances contains information as to the intramolecular potential of the molecule while the polarization dependence gives molecular orientation. The energy dependence of the near edge structures has been previously described in terms of the intramolecular bond distance[17]. Here we examine the polarization dependence of the absorption coefficient. Figure 1 presents the coordinates utilized in the following discussion. It has been shown[16,18] that for linear molecules such as CO the polarization dependence for dipole allowed transitions from an s initial state into a pure π^* state shows a $\sin^2\delta$ dependence on the angle δ between the electric field vector and the molecular axis. In general, for dipole allowed transitions from a spherically symmetric initial state to a final state with a nodal plane through the center of the initial state the absorption coefficient goes as $\cos^2\delta$ of the angle, δ, between the electric vector and the normal to the nodal plane. The polarization dependence of the dipole allowed transitions can be obtained by examining the spherical harmonic components centered on the initial state of the dipole matrix element integral. The initial state is a 1s orbital and thus has Y_o^o symmetry. The dipole operator has Y_1^m symmetry. Thus only final state components with Y_1^n symmetry will contribute to the absorption. If a node goes though the final state then only one Y_1^n is nonzero and thus the absorption coefficient goes as the $\cos^2$ of the angle between $\vec{E}$ and the normal to the nodal plane.

Thus for transitions into bound molecular states NEXAFS shows an

absorption maximum when the electric field vector (and thus the initial p-wave of the excited 1s electron if this were a photoemission event) is directed along the atomic p orbital component (centered on the excited atom) of the final state molecular orbital.

We shall consider two types of unsaturated center. Many molecules with sp hybridization (e.g. carbon monoxide) have (local) $C_{\infty v}$ symmetry, and excitations into the π^* final states are equivalent in the plane perpendicular to the bond axis. The π^* orbitals of sp^2 hybridized molecules (e.g. pyridine) by contrast, are made up of the atomic p orbitals perpendicular to the σ bonding plane (there are sp hybridized molecules with inequivalent π^* states [e.g. ketene H_2CCO] and the π^* resonances are treated independently similarily to sp^2 centers). Thus the expression describing the observed polarization dependence of the π^* transition must be modified from that used for linear molecules. Adsorbates chemisorbed on well defined crystal surfaces exist as domains that have the same rotational symmetry as the crystal substrate, i.e. for an fcc (111) surface there are 6 equivalent possible domains for the adsorbate. Therefore $\vec{M}$ in figure 1 will be found in 6 different directions, rotated by 60° about the z axis. It can be shown for crystals with threefold symmetry or greater that the sum of $\cos^2\delta$ with $\vec{M}$ rotated into the equivalent directions is invariant under rotation of the crystal about the z axis[16,19]. Thus the sum over the domain directions can be replaced by an integral over ϕ and so the expression describing the transition probability for 1s to π^* transitions is (using definitions from figure 1)[19,20]:

$$A\int_0^{2\pi} \sin^2(\delta)\,d\phi = A\int_0^{2\pi} (1-(\vec{E}\cdot\vec{M})^2)\,d\phi = A\pi(2-2\cos^2(\theta)\cos^2(\alpha)-\sin^2(\theta)\sin^2(\alpha)) \quad \text{Eq.1}$$

for sp hybridized molecules (e.g. CO) and

$$B\int_0^{2\pi} \cos^2(\delta)\,d\phi = B\int_0^{2\pi} (\vec{E}\cdot\vec{M})^2\,d\phi = B\pi(2\cos^2(\theta)\cos^2(\alpha)+\sin^2(\theta)\sin^2(\alpha)) \quad \text{Eq.2}$$

for sp^2 hybridized molecules (e.g. pyridine) where A and B are constants describing the absolute transition intensity.

For aromatic molecules we have found that the NEXAFS spectra of the adsorbed molecule are only weakly perturbed in the energy position of the peaks relative to the spectra of the condensed multilayer (Figs. 4 and 6). We therefore will use the oriented free molecule model and the $\cos^2\delta$ relation of the π^* transition to determine the angle α of the ring with respect to the surface. This involves integrating the π^* peak intensity at normal photon incidence and dividing by the integral of the π^* intensity at grazing (in our experiments 20^o) photon incidence. The spectra were normalized by dividing by clean Pt(111) spectra at the appropriate angle and the intensity before the onset of 1s excitation, i.e. the lowest scanned energy, was set to 1. The observed peak ratio is compared with the theoretical ratio presented in figure 2. The theoretical peak intensity ratio R for the π^* transitions for a photon angle θ_1 divided by that for a photon incidence angle θ_2 for sp^2 hybridized systems is given by:

$$R = \frac{(2\cos^2(\theta_1)\cos^2(\alpha)+\sin^2(\theta_1)\sin^2(\alpha))}{(2\cos^2(\theta_2)\cos^2(\alpha)+\sin^2(\theta_2)\sin^2(\alpha))} \qquad \text{Eq.3}$$

For $\theta_1 = 90^o$ and $\theta_2 = 20^o$ we obtain:

$$R = \frac{(\sin^2(\alpha))}{(0.177+1.6949\cos^2(\alpha))} \qquad \text{Eq.4}$$

In accord with previous work and in agreement with what is found for pyridine coordination complexes we will consider only those possible pyridine geometries with the nitrogen atom coordinated to the metal surface[21].

EXPERIMENTAL:

The Pt(111) crystal was cleaned by exposure to 10^{-7} torr oxygen at 870K followed by annealing under vacuum to 1200K with argon ion sputtering when required. The sample's cleanliness and order were monitored with Auger and

low energy electron diffraction spectrometry. Thermal desorption curves were obtained utilizing a heating rate of 25 degrees/second and mass spectrometric detection. The NEXAFS spectra were taken at beam line I-4 at the Stanford Synchrotron Radiation Laboratory using a grasshopper monochromator and partial electron yield detection was used to determine the absorption coefficient. The energy calibration of the monochromator was checked by monitoring the position of adsorption features due to carbon and nitrogen contamination of the optics and was found to be consistent to $\pm$0.5eV. The base pressure of the system before the experiment was ~ $1*10^{-10}$.

RESULTS:

The thermal desorption curves of perdeuterated pyridine are shown in figure 3. Three deuterium[22] desorption peaks were observed with area ratios of approximately 1:2:2, similar to that reported for Ni(100)[2]. Pyridine multilayer desorption occurred at ~200K with a tail on the pyridine desorption peak extending to 370K. These results will be discussed with the associated NEXAFS spectra.

The pyridine chemisorption states were prepared by condensing a multilayer ice on the Pt(111) surface and annealing to sequentially higher temperatures. Deposition of a multilayer ensures that the sample is dosed to saturation coverage. By sequentially annealing to higher temperatures one can observe intermediates while eliminating the ambiguity introduced by preparing new samples for each measurement. Since many of the molecules investigated do not have x-ray absorption spectra available for the gas phase, the spectra of the multilayer state also offer the advantage that they can serve as pseudo gas phase "standards" since they are generally close to the spectra observed for the gas phase[23].

The multilayer NEXAFS spectra for pyridine are shown in figure 4. Both

carbon K edge and nitrogen K edge spectra were recorded. The sample was prepared by condensing $6*10^{-6}$ torr-seconds (6 Langmuir or 6L) on the Pt(111) surface held at 90K. The spectra show almost no polarization dependence, suggesting that the orientation of the pyridine molecules in the ice is isotropic. Peaks A and B are π^* transitions, and the peaks C and D are σ transitions. The π resonances are sharper than those for the subsequent monolayer states due to the longer lifetime of the resonances for molecules in the multilayer matrix, with small overlap with the metal states (equivalently the broadening for molecules chemisorbed on metal surfaces is due to mixing of metal states into the molecular states). This also explains why for aromatic rings with the π system coordinated to the surface the π resonance width is greater than when the π system is tilted away from the surface (see for example the spectra in reference 14).

Annealing the multilayer (6L) sample shown in figure 4 to 240K momentarily and cooling to 90K yields the spectra shown in figure 5. This case shows a π^* resonance that predominates at grazing photon incidence ($\vec{E}$ near normal). Analysis of the π^* region gives a ratio of I_{90}/I_{20} of 0.57 for the carbon edge and 0.83 for the nitrogen edge. A smooth background was subtracted to generate the peak areas. This and the uncertainty in the degree of polarization of the photon beam (effective polarization from 85% along the plane of the synchrotron ring[16] and up) gives an uncertainty of 20% ($\pm$0.11 for the carbon edge $\pm$0.15 for the nitrogen edge) in the ratio and an apparent tilt angle α of 52 ± 6 degrees (averaged over multiple determinations of angle). Previously, several geometries have been suggested for pyridine chemisorbed on group 8 metals. On Ag(111) a low temperature, high coverage, state with a tilt angle α of approximately 55° to the surface has been proposed[10,11]. However, we have investigated a number of different annealing schemes and find that the conversion from the tilted to the perpendicular state occurs as low

as 240K (albeit slowly). Thus the spectra at 240K may show some degree of conversion to the perpendicular state so the actual tilt angle α of the ring for the low temperature form may be smaller than 52 ± 6^{o} [24]. Note that 240K is in the region of the desorption tail of molecular pyridine from Pt(111) and thus there may be some contribution due to coverage in the observed ring tilt.

Figure 6 shows spectra from pyridine dosed at room temperature to saturation (~24L) , followed by a momentary anneal to 320K, with the spectra taken at room temperature. The large π^* resonance at normal photon incidence ($\vec{E}$ parallel to the surface) and large σ resonance at grazing incidence ($\vec{E}$ near normal to the surface) are consistent with a perpendicular orientation for the ring. Analysis of the π^* resonance gives a ratio of $6.0\pm50\%$ (±3.0) for the carbon edge and $9.3\pm50\%$ (±4.7) for the nitrogen edge giving an angle α of 85 ± 10 degrees.

Figure 7 shows the sample of figure 5 after annealing to 410K (past the first hydrogen desorption) and cooling to 90K. A state very similar to figure 6 is observed, i.e. a perpendicular coordination state. Analysis gives a ratio of $3.0\pm30\%$ (±0.9) for the carbon edge and $2.5\pm30\%$ (±0.8) for the nitrogen edge which indicates an angle α of 74 ± 10 degrees (averaged over multiple determinations of angle).

DISCUSSION:

The question of the reversablity of the transformation from the tilted to the perpendicular state has been of interest[3,4]. When spectra were taken at elevated temperatures (for example, figure 6) they systematically indicate ring angle α closer to perpendicular. This increase in apparent angle would be produced by a reversible conversion of about 10% of the perpendicular form to a tilted form at 90K, which is at the limit of the reliability of the measurement and data analysis.

The thermal desorption of pyridine shows the loss of one hydrogen equivalent at 370K. The desorption temperature of hydrogen adsorbed on clean Pt(111) is 350-370K. We infer that the observed low temperature hydrogen peak is desorption limited and thus the C-H cleavage that generates it occurs at or below room temperature. This leads to the assignment of the high temperature pyridine chemisorption state shown in figures 6 and 7 to the previously suggested[13] alpha pyridyl form. Thus we propose that the conversion to the perpendicular form at higher temperatures is motivated by the formation of a metal carbon bond.

In Fig. 8 we present a dynamic picture of pyridine chemisorption on Pt(111) as a function of temperature. Pyridine forms a disordered multilayer on chemisorption at 90K. On annealing the multilayer to progressively higher temperatures the multilayer evaporates and a monolayer with a tilted ($\alpha \leq 52^{o}$) pyridine ring is formed. Slowly at 240K and more rapidly at higher temperatures the alpha C-H bond is cleaved and the pyridine is converted to an alpha pyridyl state characterized by the ring becoming perpendicular to the surface. This transformation may be reversible to an extent of approximately 10%[25].

ACKNOWLEDGEMENTS:

One of us (A. L. J.) wishes to thank Dr David A. Shirley for helpful discussions and a critical reading of the manuscript. A. L. Johnson and E. L. Muetterties (deceased) wish to acknowledge the support of the National Science Foundation and the Chemical Sciences Division of the U. S. Department of Energy under Contract No. DE-AC03-76SF00098. The work reported here was done at the Stanford Synchrotron Radiation Laboratory which is supported by the Office of Basic Energy Sciences of DOE and the Division of Materials Research of the National Science Foundation.

BILBLIOGRAPHY / FOOTNOTES:

1. Wexler, R. M.; Tsai, M-C; Friend, C. M.; and Muetterties, E. L. J. Am. Chem. Soc., 104, 2034 (1982)

2. Robota, H.J.; Whitmore, P. M.; and Harris, C. B. J. Chem. Phys., 76(4), 1692 (1982)

3. Avouris, Ph.; DiNardo, N. J.; and Demuth, J. E. J. Chem. Phys., 80(1), 491 (1984)

4. DiNardo, N. J.; Avouris, Ph.; and Demuth, J. E. J. Chem. Phys., 81(4), 2169 (1984)

5. Bandy, B. J.; Lloyd, D. R.; and Richardson N. V. Surf. Sci., 89, 344 (1979)

6. Nyberg, G. L. Surf. Sci., 95, L273 (1980)

7. Mate, M. and Somorjai, G. A. Proceedings First Internat. Conf. on the Structure of Surfaces (ICSOS I) August 1984, Berkeley CA. Springer Series in Chemical Physics (to be published)

8. Netzer, F. P. and Mack, P. Chem. Phys. Lett., 95(6), 492 (1983)

9. Netzer, F. P. and Mack, P. J. Chem. Phys., 79(2), 1017 (1983)

10. Demuth, J. E.; Christmann, K.; and Sanda, P. N. Chem. Phys. Lett., 76(2), 201 (1980)

11. Avouris, Ph. and Demuth, J. E. J. Chem. Phys., 75(10), 4783 (1981)

12. Netzer, F. P., Bertel, E.; and Mathew, J. A. D. Surf. Sci., 92, 43 (1980)

13. Gland, J. L. and Somorjai, G. A. Surf. Sci., 38, 157 (1973)

14. Johnson, A. L.; Muetterties, E. L.; and Stöhr, J. J. Am. Chem. Soc., 105, 7183 (1983)

15. Richardson, N. V. Proceedings First Internat. Conf. on the Structure of Surfaces (ICSOS I) August 1984, Berkeley CA. Springer Series in Chemical Physics (to be published)

16. Stöhr, J. and Jaeger, R. Phys. Rev. B, 26, 4111 (1982)

17. Stöhr, J., Sette, F., and Johnson, A. L. Phys. Rev. Lett., 53, 1684 (1984)

18. Wallace, S. and Dill, D. Phys. Rev. B, 17, 1692 (1978)

19. Stöhr, J. in preparation

20. It is interesting to note that Eq.1 can be rendered in the form:
$I=C[1-1/4(3\cos^2\theta -1)(3\cos^2(\alpha)-1)]$
and Eq.2 in the form:
$I=D[1+1/2(3\cos^2\theta -1)(3\cos^2(\alpha)-1)]$
and thus at α or θ angles of 54.7° (magic angle) there is no polarization dependence to the resonances.

21. We observe a shift in the position of the π^* resonance at the nitrogen edge of +2 eV when the pyridine is annealed to the high temperature state. This can be rationalized by invoking a repulsive dipole - dipole interaction between the molecular dipole (formed by the nitrogen core hole and the electron in the π^* orbital) and the surface dipole (formed from the electron density in space above the metal surface) which is consistent with the nitrogen down geometry.

22. The thermal desorption curves of perdeuterated pyridine rather than normal pyridine are presented to obviate the concern over background hydrogen contamination. We have found for pyridine that the hydrogen peaks shift by no more than 12 degrees on deuteration.

23. We have prepared ices of benzene and compared them to the gas phase electron scattering results (see Hitchcock, A. P. and Brion, C. E. J. Electron Spectrom. and Rel. Phenom. 10, 317, (1977)) and found close agreement. This is expected to be generally true (see for example Dehmer, J. L., Dill, D. and Parr, A. C. in "Photoionization Dynamics of Small Molecules" in Photophysics and Photochemistry in the Vacuum Ultraviolet edited by McGlynn et. al.)

24. If the chemisorption state of figure 5 were not mixed then one would expect that the π^* transition would have the same width at all electric field vector directions. The observed greater width of the resonance with grazing photon incidence suggests a mixed state, but the possible overlap of peak B with peak A precludes further analysis.

25. It is interesting to note that for high coverages a pyridine desorption is evident at higher temperatures (~470K) and thus disporportionation of the pyridine might be invoked to provide for a small degree of reversibility of the formation of the alpha pyridyl. More detailed thermal desorption studies and EELS results will be presented by Grassian, V. and Muetterties, E. L. (in preparation).

26. The gas phase 1s binding energy relative to the vacuum level of carbon in pyridine is not known but should be between 290.2eV (C 1s for C_6H_6[27a]) and

293.5ev (C 1s for HCN[27b]); the nitrogen 1s binding energy in pyridine is 404.9eV[27c]. Resonances below the binding energy are bound state resonances. For chemisorption states the onset of absorption corresponds to excitation to the Fermi level of the metal. Thus the region from the onset of absorption to the onset plus the work function are resonances below the photoemission threshold and correspond to the bound molecular resonances. The work function of pyridine covered Pt(111) for saturation coverage at 278K is approximately 3 volts[13].

27. a:Gelius, U.; Allan, C. J.; Johansson, G.; Siegbahn, H.; Allison, D. A.; and Siegbahn, K. Phys. Scripta, 3, 237 (1971) b:Davis, D. W.; Hollander, J. M.; Shirley, D. A.; and Thomas, T. D. J. Chem. Phys., 52, 3295 (1970) and Thomas, T. D. and Shaw, Jr., R. W. J. Electron Spectrosc. and Relat. Phenom., 5, 1081 (1974) c:Brown, R. S.; Tse, A.; and Vederas, J. C. J. Am. Chem. Soc., 102, 1174 (1980) and Brown, R. S. and Tse, A. Can. J. Chem., 58, 694 (1980)

FIGURE 1.

Coordinate system for the analysis of the polarization dependence of NEXAFS spectra of unsaturated molecules. In the case of pyridine the molecular symmetry axis ($\hat{n}$ vector) is along the ring normal. In general, for excitations at unsaturated centers the molecular symmetry axis is along the bond axis for sp hybridized systems and perpendicular to the bonding plane for sp^2 systems.

FIGURE 2

The theoretical peak ratio of the intensity of the π^* transitions for normal and 20^o photon incidence for sp^2 hybridized systems.

FIGURE 3.

Thermal desorption spectra of perdeutero-pyridine. Pyridine was dosed at 170K and $0.33*10^{-6}$ torr-second (0.33 Langmuir or 0.33L) background pressure with a needle doser and thus the coverage is approximately half of saturation.

FIGURE 4.

The NEXAFS spectra for an approximately 6 layer multilayer of pyridine on Pt(111) (assuming sticking coefficient of 1). Section I is the carbon K edge and section II is the nitrogen K edge. Peaks A and B are π^* transitions, and the peaks C and D are σ transitions[26]. These spectra were taken with normal incidence photons.

FIGURE 5.

NEXAFS spectra of pyridine chemisorbed on Pt(111). The sample was prepared from the multilayer of figure 4 by momentarily heating to the indicated temperature. Note the strong π^* transition at grazing photon incidence (near normal electric vector) and strong σ transitions at normal

photon incidence (parallel electric vector) for both carbon and nitrogen K edges, consistent with a pyridine tilt angle α of 52 ± 6 with respect to the surface.

FIGURE 6.

The NEXAFS spectra of 24L of pyridine deposited on Pt(111) at room temperature and momentarily annealed to the indicated temperature. Note the strong π^* transition at normal photon incidence (parallel electric vector) and the strong σ transitions at grazing photon incidence (electric vector near normal), consistent with a pyridine ring perpendicular to the surface.

FIGURE 7.

NEXAFS spectra of pyridine chemisorbed on Pt(111). Preparation was as for figure 5, with an added anneal to 410K. Note the similarity with figure 6.

FIGURE 8

Proposed chemisorption states for pyridine on Pt(111). The diagrams on the left show the electric field direction that yield the NEXAFS spectra presented earlier. State I corresponds to Figure 4. State II corresponds to Figure 5 (assuming an unmixed state). State III corresponds to Figures 6 and 7. Thus, for example, the alpha pyridyl state of III should have a large π^* transition for parallel electric field vector (diagram a) and we should see a large π^* peak for figures 6a and 7a.

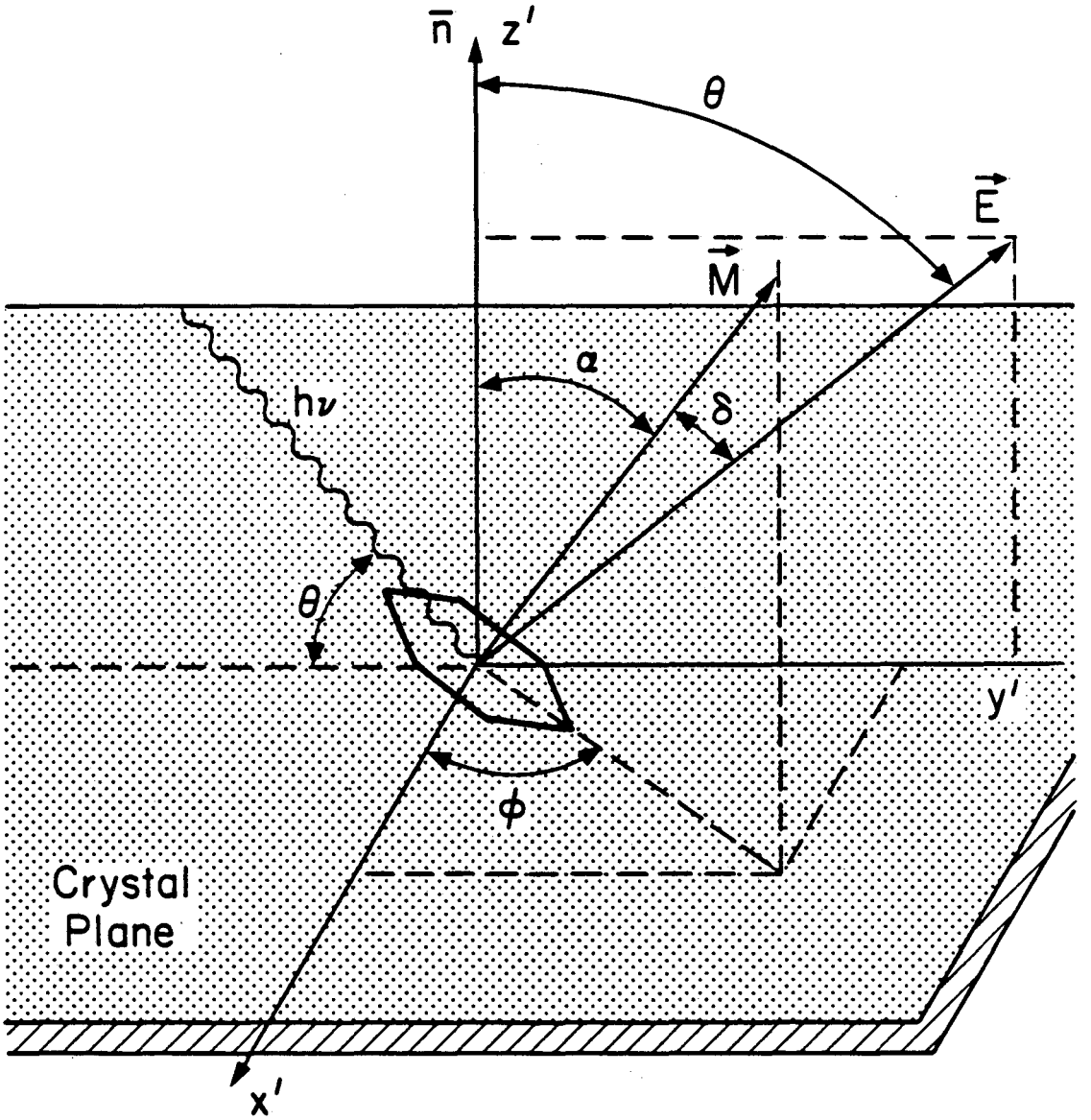
n̄
z′
θ
E⃗
M⃗
α
δ
hν
θ
y′
ϕ
Crystal Plane
x′
n̄ Surface Normal
M⃗ Molecular Symmetry Axis
E⃗ Electric Field Vector
XBL 852-1102

Figure 1

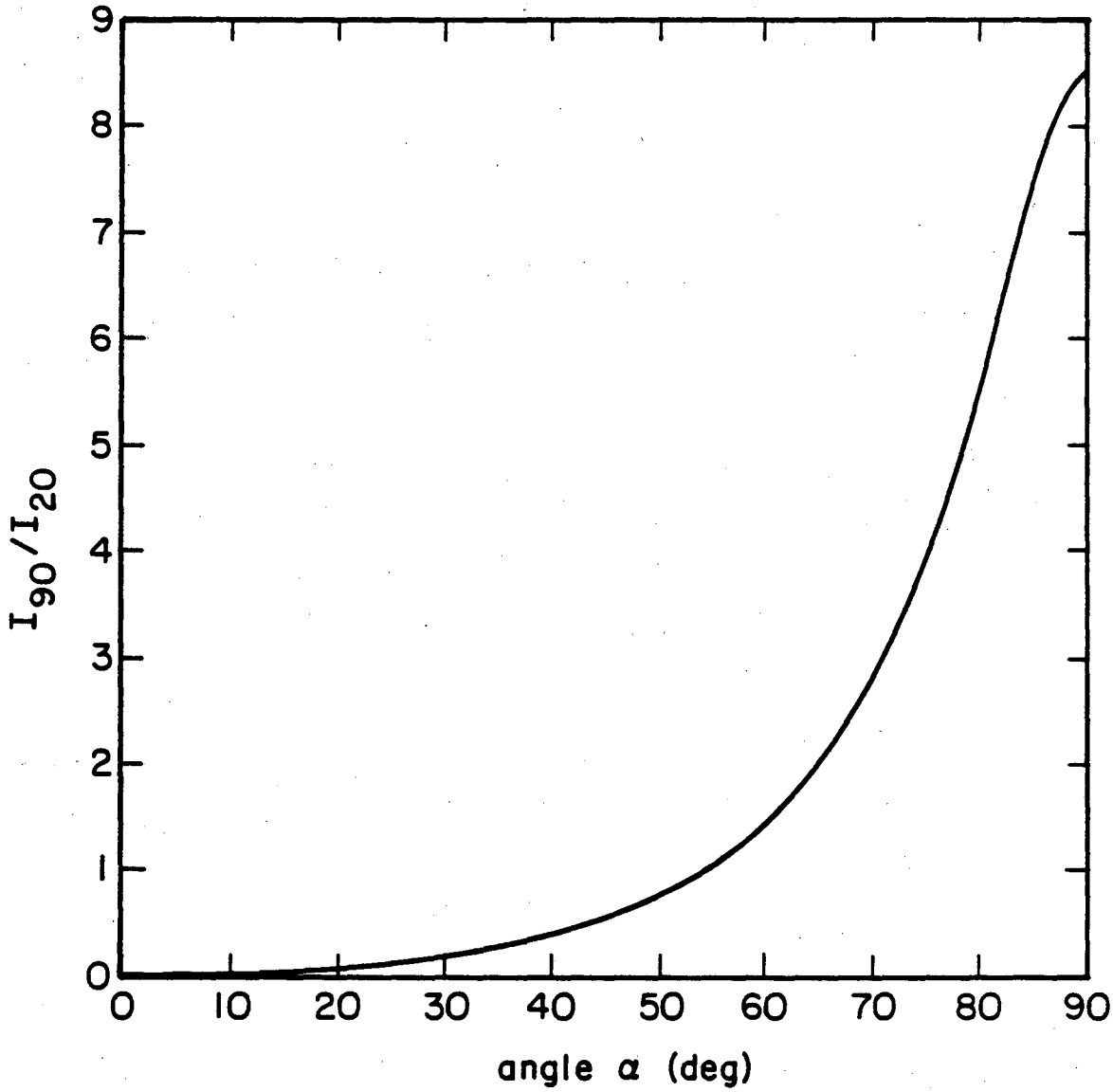

XBL 852-1101

Figure 2

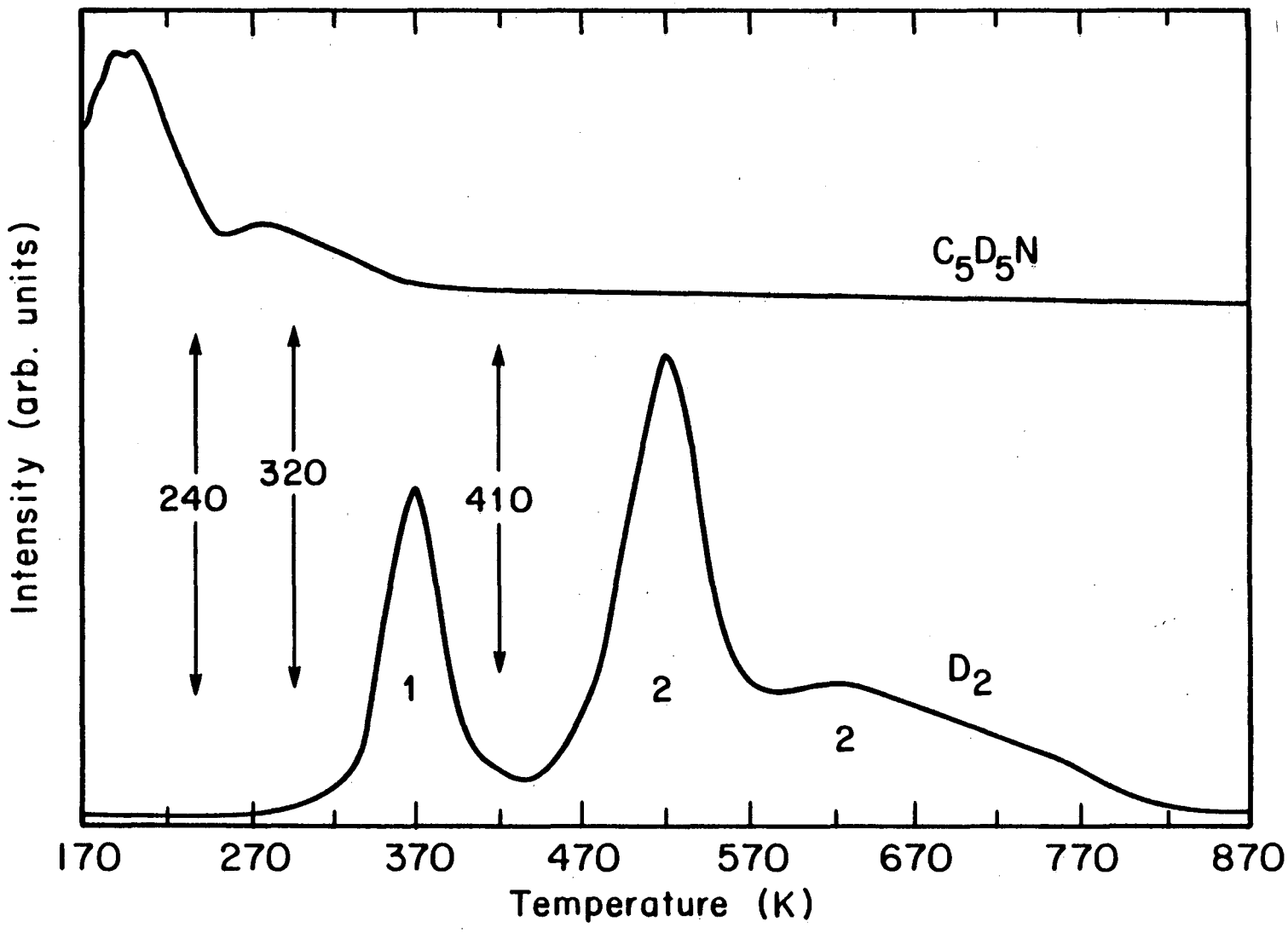

XBL 852-1096

Figure 3

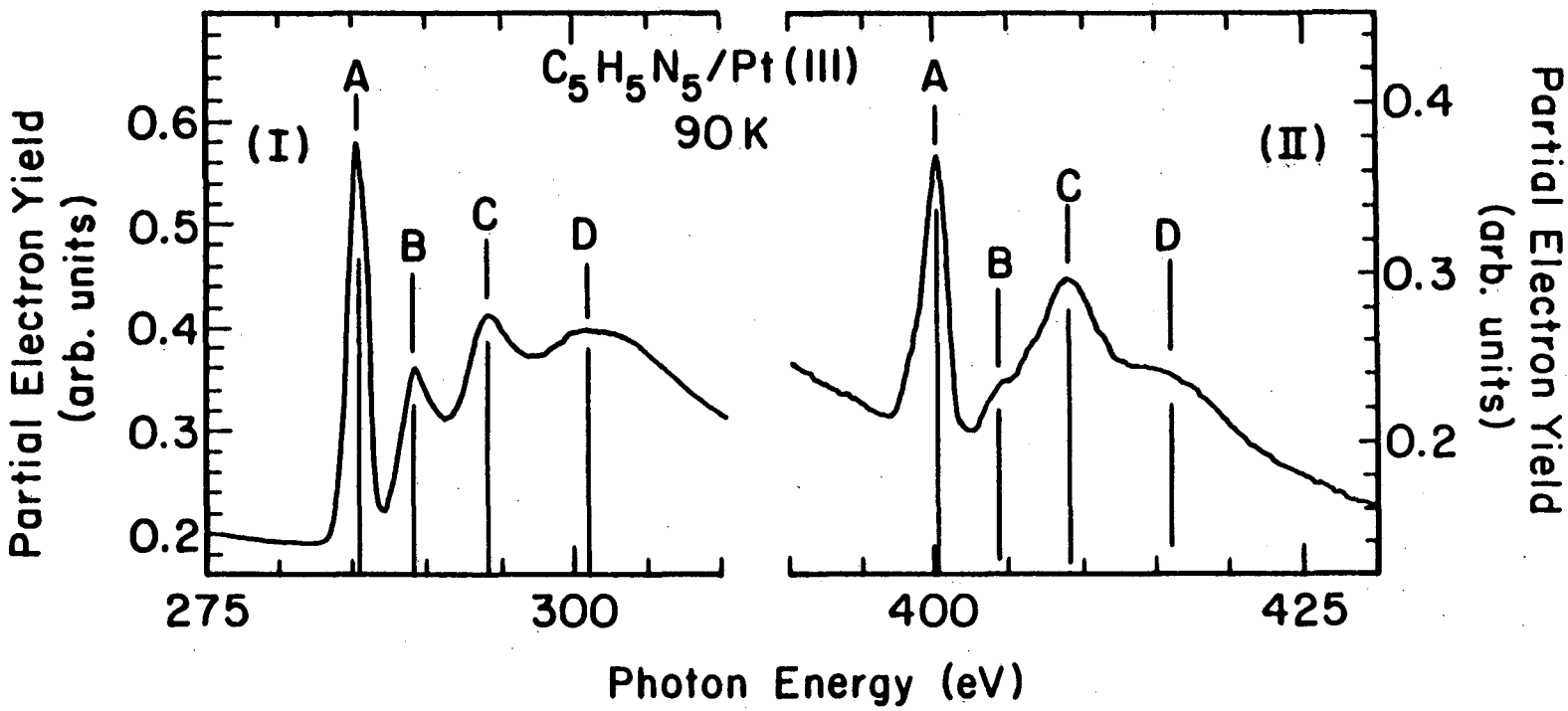

XBL 852-1095

Figure 4

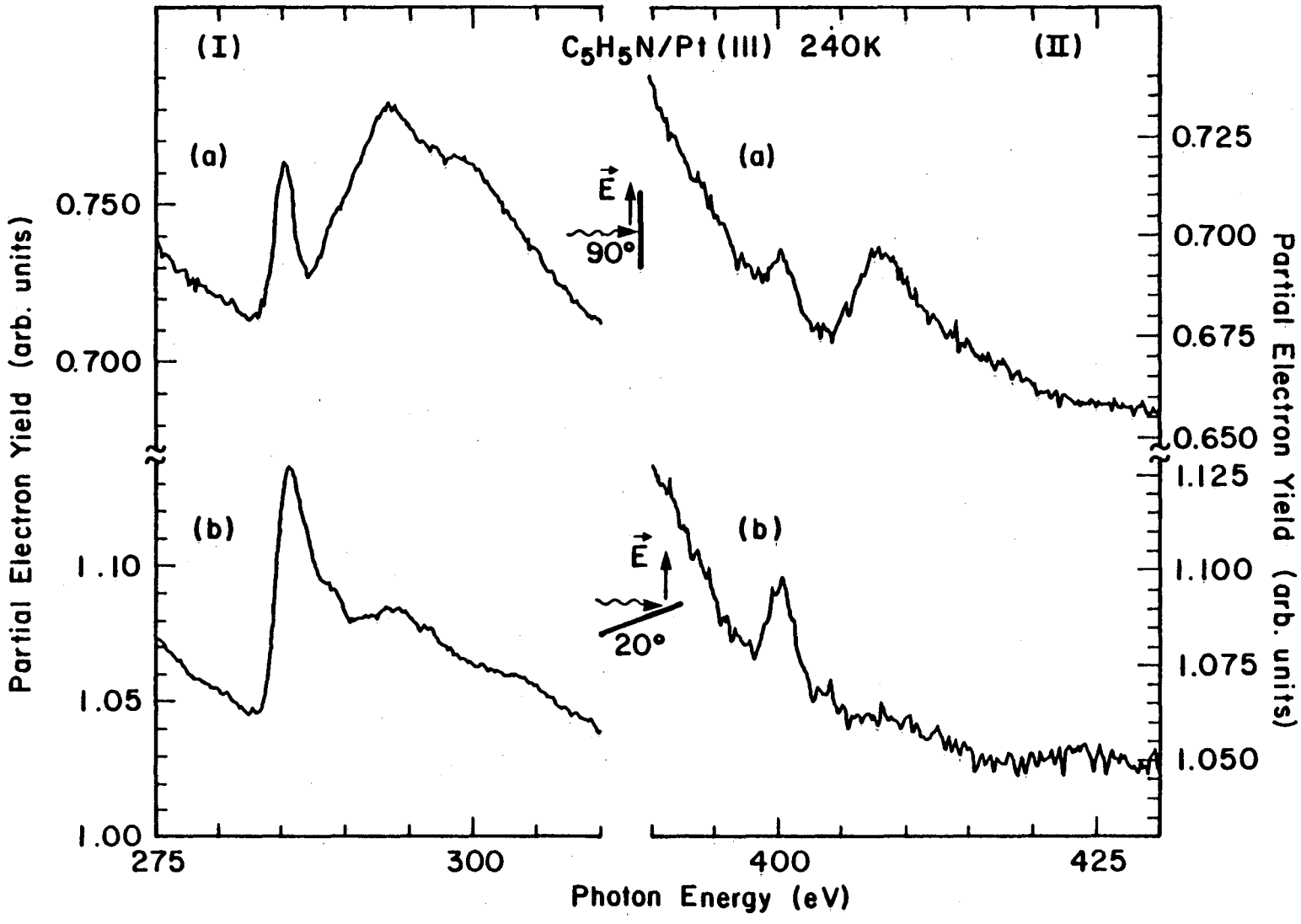

Figure 5

XBL 852-1097

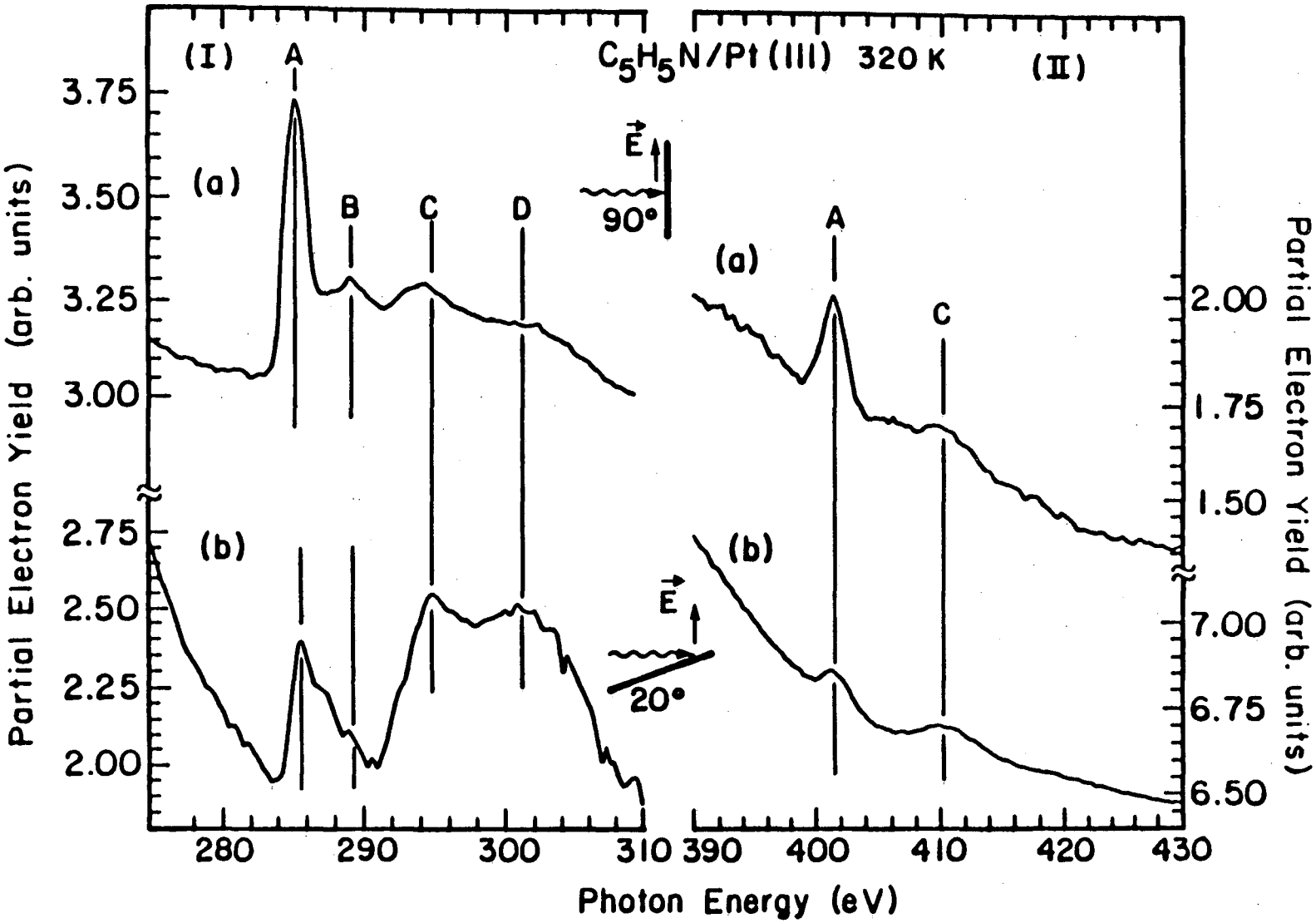

XBL 852-1098

Figure 6

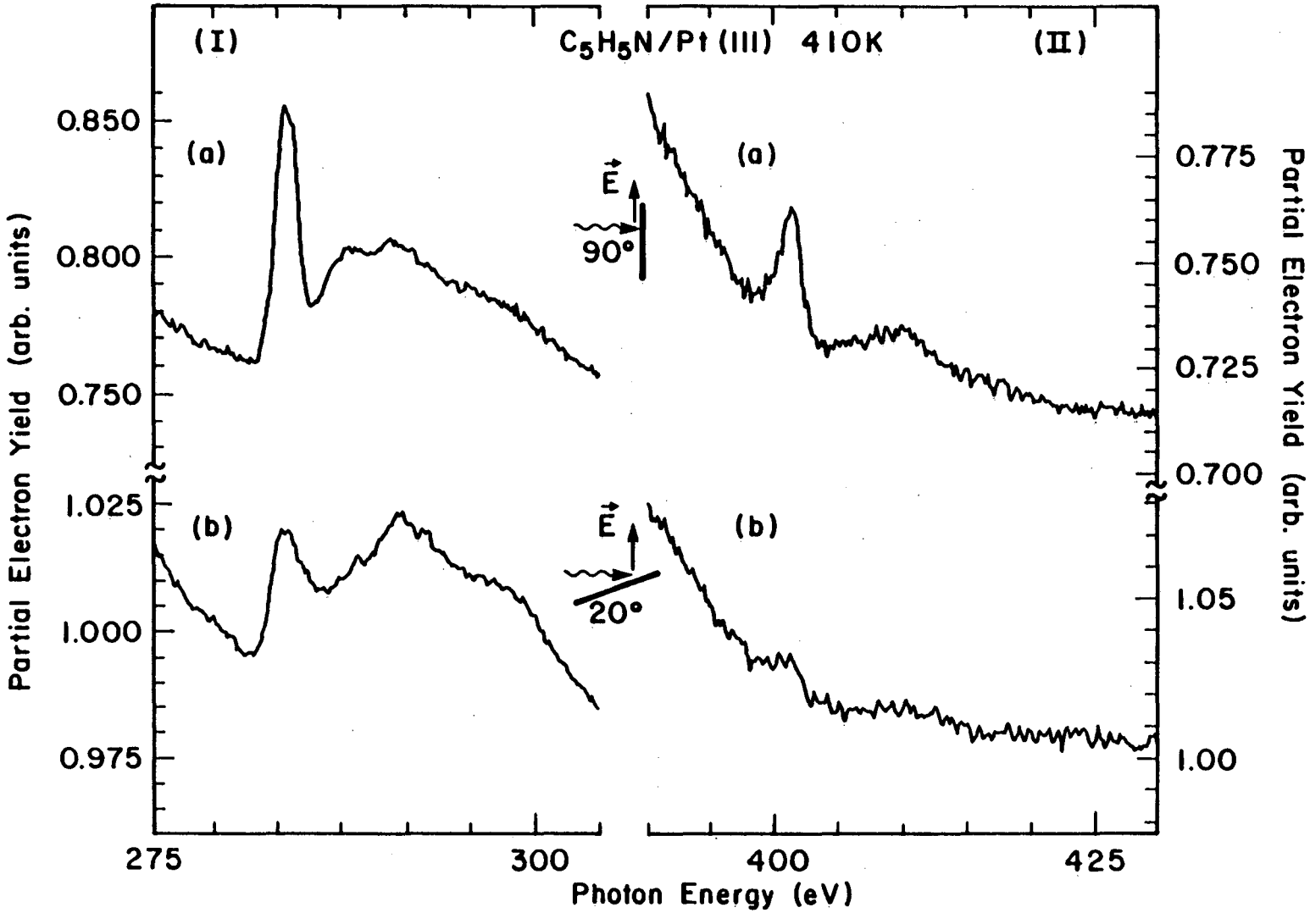

XBL 852-1099

Figure 7

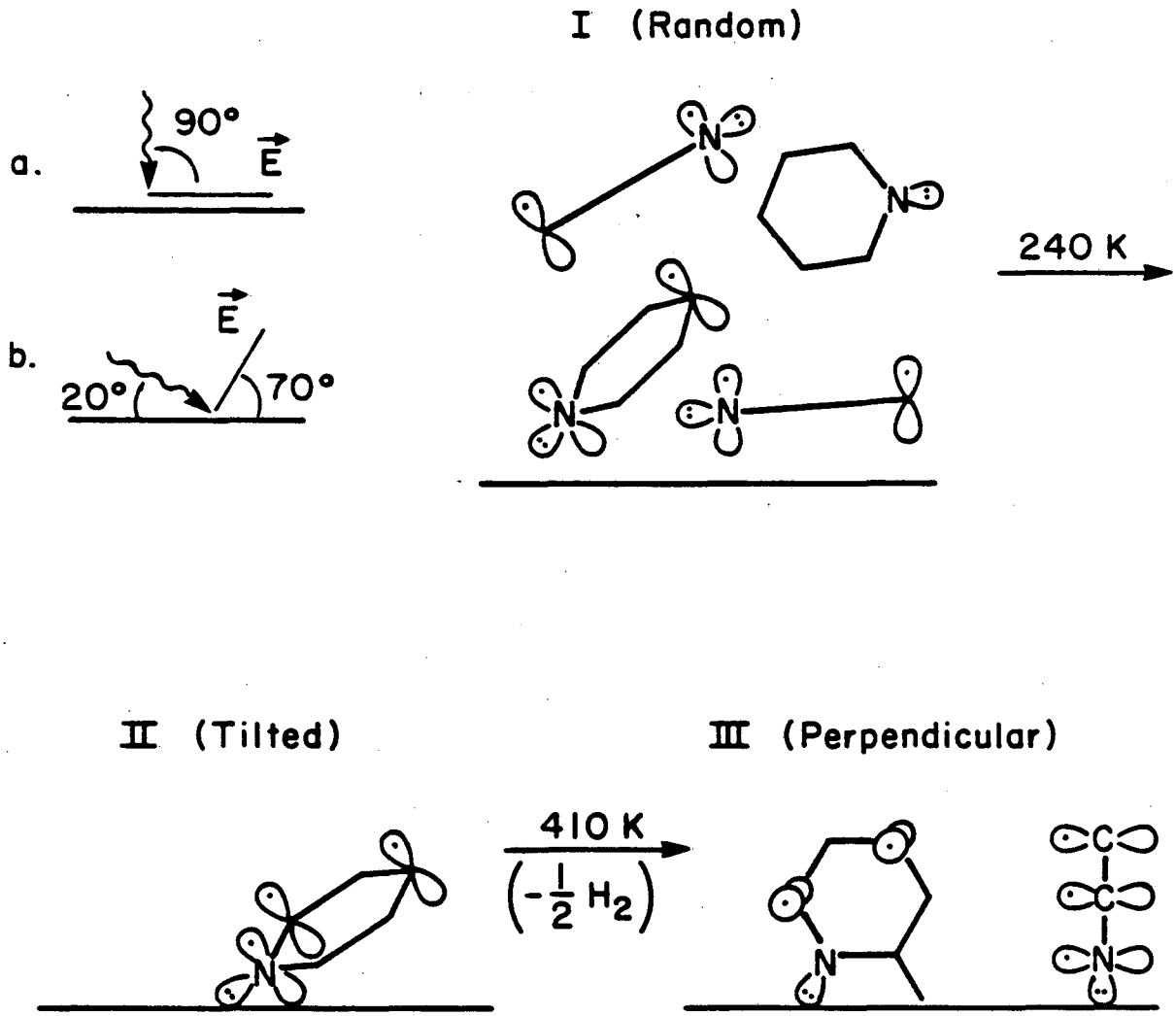
I (Random)
a.
90°
E
b.
E
20°
70°
240 K
II (Tilted)
III (Perpendicular)
410 K
(-½ H2)
XBL 852-1100

Figure 8

This report was done with support from the Department of Energy. Any conclusions or opinions expressed in this report represent solely those of the author(s) and not necessarily those of The Regents of the University of California, the Lawrence Berkeley Laboratory or the Department of Energy.

Reference to a company or product name does not imply approval or recommendation of the product by the University of California or the U.S. Department of Energy to the exclusion of others that may be suitable.

TECHNICAL INFORMATION DEPARTMENT
LAWRENCE BERKELEY LABORATORY
UNIVERSITY OF CALIFORNIA
BERKELEY, CALIFORNIA 94720